ELSEVIER

Journal of Alloys and Compounds 330–332 (2002) 338–341

Journal of ALLOYS AND COMPOUNDS

www.elsevier.com/locate/jallcom

Dihydride transmission quenching in switchable $La_{1-z}Y_zH_x$ mirrors

A.T.M. van Gogh*, R. Griessen

Faculty of Sciences, Division of Physics and Astronomy, Vrije Universiteit, De Boelelaan 1081, 1081 HV Amsterdam, The Netherlands

Abstract

Dihydrides of $La_{1-z}Y_z$ films with $0 < z < 1$ are studied by reflectance-transmittance measurements and ellipsometry in the visible and near infrared spectral range. The dihydride transmission window, present in LaH_2 and YH_2, is strongly suppressed in thin $La_{1-z}Y_zH_2$ films. By modelling the complex dielectric function of the alloys with a Drude–Lorentz parametrization we show that the suppression is due to atomic disorder, mainly via optical absorptions at energies larger than 4.5 eV.

Keywords: Switchable metal-hydride mirrors; Spectrometry; Ellipsometry; Y; La; Alloys; Dihydrides; Optical properties

1. Introduction

A metal-hydride switchable mirror consists essentially of a transparent substrate covered by a rare earth (RE) based, optically active layer of several hundred nanometers thick. This layer is capped with a thin layer of palladium that protects the highly reactive, active layer against oxidation and catalyses H_2 dissociation [1]. By changing the hydrogen concentration x, electrochemically or by gas phase loading, all RE metals and many RE based alloys can be switched reversibly from metallic, reflective ($x \approx 2$) to insulating, transparent ($x \approx 3$) [2–4], and therefore have a high technological potential [5].

A peculiar optical property of YH_2 and LaH_2 is that, although these materials are low resistivity metals, they are slightly transparent in the red and near infrared part of the optical spectrum. In this work we show that this transmission window exists in $La_{1-z}Y_zH_2$ alloys too, but that its magnitude is strongly suppressed for intermediate z. By a Drude–Lorentz analysis of experimental complex dielectric functions, we identify the origin of the suppression.

2. Samples

$La_{1-z}Y_z$ films of 300 nm thickness are made at room temperature and under ultra high vacuum conditions ($\sim 10^{-9}$ Pa) by e-gun co-deposition of the parent metals (99.9% purity) on quartz glass substrates. For $z > 0.5$ the $La_{1-z}Y_z$ films are covered by 15 nm Pd, whereas for $z < 0.5$ we use a composite cap layer, consisting of 1.5 nm AlO_x covered with 15 nm Pd [6]. In every evaporation two extra samples are made for composition and thickness measurements using Rutherford backscattering spectrometry and profilometry. From these analyses we find z to be accurate to 2 at.% and film thicknesses to 2%. We detect oxygen contaminations up to a few at.%.

For (near normal) reflectance-transmittance ($R - T$) measurements between 0.72 eV and 3.5 eV, the sample is mounted in a gas loading cell that is placed in a Bruker IFS 66/S Fourier-transform infrared spectrometer equipped with a $R - T$ accessory.

For the determination of the complex dielectric function $\varepsilon(\omega)$, we use ellipsometry. This technique has the advantage that it is rather insensitive to the film thickness of the strongly absorbing dihydrides, contrary to transmittance measurements. We use a rotating-analyzer ellipsometer (VASE, J.A. Woollam Co., Inc.) that measures the ratio of the complex Fresnel reflection coefficients

$$\frac{r_p}{r_s} = \tan \Psi \exp i\Delta \tag{1}$$

in terms of the ellipsometric quantities $\Psi(\omega)$ and $\Delta(\omega)$ in the spectral range $0.75 \leq \hbar\omega \leq 4.5$ eV. The subscripts refer to the polarizations parallel (p) and perpendicular (s) to the plane of incidence. The complex dielectric function $\varepsilon(\omega)$ of the $La_{1-z}Y_zH_2$ layers is obtained by numerical inversion of $\Psi(\omega)$ and $\Delta(\omega)$. As substrates we use quartz prisms with a top angle of 40° and with the film evaporated on the base. By measuring under 70° the incident angle on the air-quartz interface is 90°, which greatly simplifies the numerical inversion. We hydrogenate the samples electrochemically and in situ.

---

*Corresponding author.

0925-8388/02/$ – see front matter
PII: S0925-8388(01)01539-0

It turns out that the first hydrogen loading, electrochemical or with H_2 gas, is inhomogeneous. Subsequent loadings are homogeneous and reproducible. Therefore we always switch the as-deposited sample to the trihydride and back to the dihydride before optical measurements are done.

More details about the two measuring techniques mentioned above, are given in Refs. [7–9].

3. Results and discussion

In Fig. 1 the dihydride transmittance is given for the various $La_{1-z}Y_z$ alloys. All alloys exhibit a similar dihydride transmission window. This window arises because of interband transitions below the unscreened plasmon energy $\hbar\omega_p$ that is approximately 4 eV for YH_2 and LaH_2 [10,11]. Low lying interband absorptions screen the restoring forces between fluctuations of the charge density of the conduction electrons, which shifts the plasmon energy to lower energies. This results in a narrow region where the total absorption is small and therefore the film is transparent even for rather thick films (up to several hundred nanometers). Similar effects occur at higher energies in Au and Ag.

The different nature of the optical response at low and high energies is more clearly seen in the dihydride reflectance spectra (Fig. 2). At low energies ($\lesssim 1.5$ eV) the dihydrides are highly reflective due to the free electron optical response, characteristic for metals below the plasmon energy. On approaching the (screened) plasmon frequency the reflectance sharply decreases and above the plasmon frequency ($\gtrsim 1.5$ eV) the reflectance is governed by optical interband absorptions between *d*-bands [11].

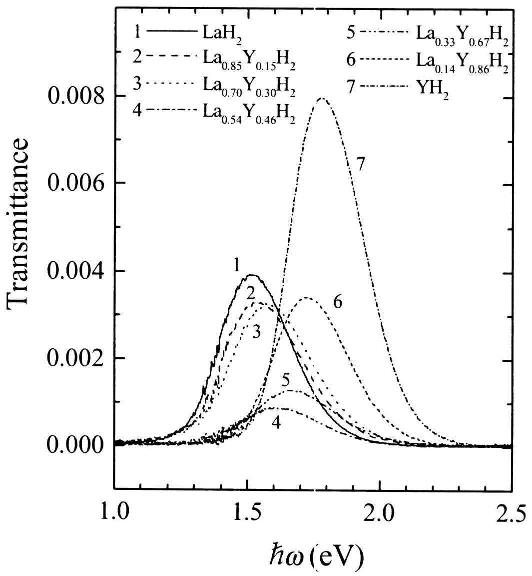

Fig. 1. Dihydride tranmission windows for $La_{1-z}Y_zH_2$ alloys. Although the transmission window is observed for all alloys, its magnitude is strongly suppressed upon alloying.

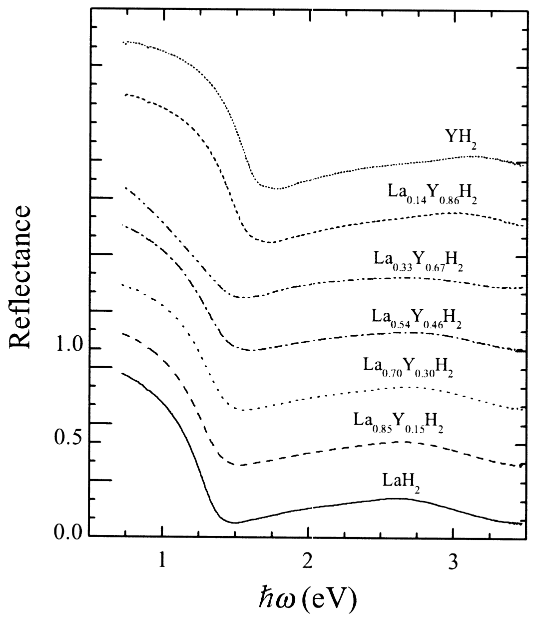

Fig. 2. Dihydride reflectance for the $La_{1-z}Y_zH_2$ alloys. For clarity we shifted the spectra with $z>0$ with multiples of 0.3. At low energies the dihydrides are strongly reflecting. However, as the (screened) plasmon energy is approached, the reflectance strongly decreases. Above the plasma edge, the reflectance is due to interband absorptions.

Fig. 3 shows the *z*-dependence of the energy $\hbar\omega_{max}$ and the dihydride transmittance T_{max} corresponding to the transmittance maximum (taken from Fig. 1). We observe a monotonic shift of $\hbar\omega_{max}$ from 1.52 eV for LaH_2 to 1.78 eV for YH_2. However, T_{max} varies in a highly non-linear way, with a minimum that is one order of magnitude lower than for YH_2 or LaH_2. The minimum occurs at $z=0.46$ which is close to $z=0.5$ where atomic disorder is maximum.

To investigate the relation between atomic disorder and

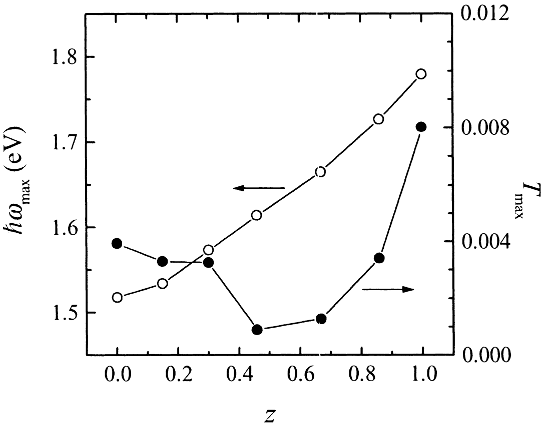

Fig. 3. Composition dependence of the photon energy $\hbar\omega_{max}$ and the transmittance T_{max} corresponding to the maximum in dihydride transmittance (see Fig. 1).

the magnitude of the dihydride transmission window, we measure the complex dielectric function $\varepsilon(\omega)$ that is more directly related to electronic properties than $R(\omega)$ and $T(\omega)$. The measured real and imaginary part of $\varepsilon(\omega)$ for three representative alloys are given in Fig. 4. The shape of $\varepsilon(\omega)$ is the same for all alloys, but characteristic features shift to higher energies for increasing z.

From X-ray diffraction we know that all $La_{1-z}Y_zH_2$ alloys are fcc and that the metal atoms form a disordered solid solution. The changes in optical properties thus result from changes in electronic properties of the material and it makes sense to model $\varepsilon(\omega)$ using a sum of one Drude and three Lorentz oscillators (LO's):

$$\begin{aligned}\varepsilon(\omega) &= \varepsilon_1 + i\varepsilon_2 \\ &= \varepsilon_\infty - \frac{\omega_p^2}{\omega^2 + i\omega/\tau} + \sum_{j=1}^{3} \frac{f_j}{\omega_{0j}^2 - \omega^2 + i\omega\beta_j},\end{aligned} \qquad (2)$$

The constant ε_∞ in Eq. (2) accounts for excitations above 4.5 eV. The second term describes the free carrier response and is of the Drude form, characterized by the plasmon frequency ω_p and the relaxation time τ. The last three terms represent the effect of interband and/or impurity absorptions. Each LO is characterized by an oscillator strength f, a resonance frequency ω_0 and a broadening parameter β. The choice for *three* LO's is supported by fit results using two and four LO's; it turns out that two LO's clearly give worse fits than three LO's, whereas fitting four LO's leads to zero strength of the fourth LO. Eq. (2) describes the optical properties well, as is demonstrated for three representative materials in Fig. 4. Similar fits are obtained for all alloys.

From the found Drude–Lorentz (DL) parametrizations of $\varepsilon(\omega)$ we calculate the transmittances of a 15 nm Pd/300 nm $La_{1-z}Y_zH_x$/Suprasil stack [12] and the resulting $T_{max}(z)$ and $\hbar\omega_{max}(z)$ are shown in Fig. 5 (solid circles). Although the calculated values of T_{max} are somewhat underestimated, we conclude that the suppression is well reproduced by the DL parametrization.

We examine the effect of atomic disorder on $\varepsilon(\omega)$ by fitting the z-dependence of each DL parameter to the second-order polynomial $y(z) = y(0) + [y(1) - y(0)] \cdot z + 4y_{do} \cdot z(z-1)$, with $y(0)$, $y(1)$ and y_{do} constants. Atomic disorder is represented by the third term (it is maximum at $z = 0.5$). We find that y_{do} significantly differs from zero only for $\varepsilon_\infty(z)$, the resonance frequencies $\omega_{0i}(z)$ and the

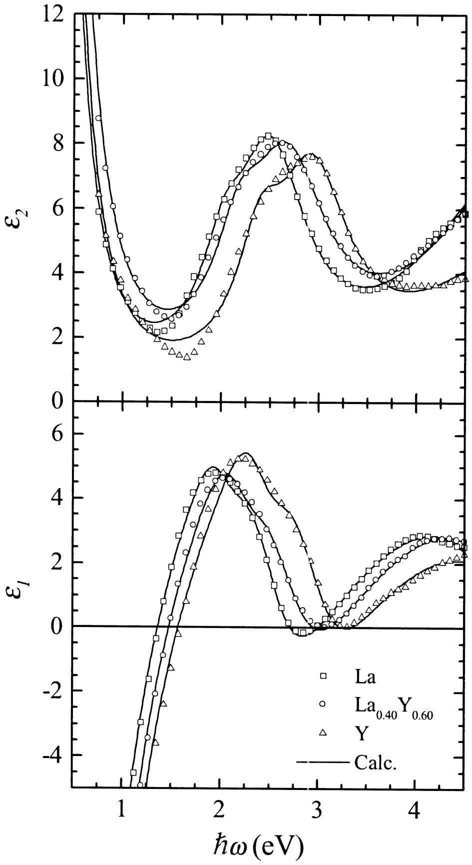

Fig. 4. Measured $\varepsilon(\omega)$ for LaH_2, $La_{0.40}Y_{0.60}H_2$ and YH_2 (symbols) and the result of the Drude-Lorentz fits (lines). For clarity results are shown for only three alloys and not all data points are plotted.

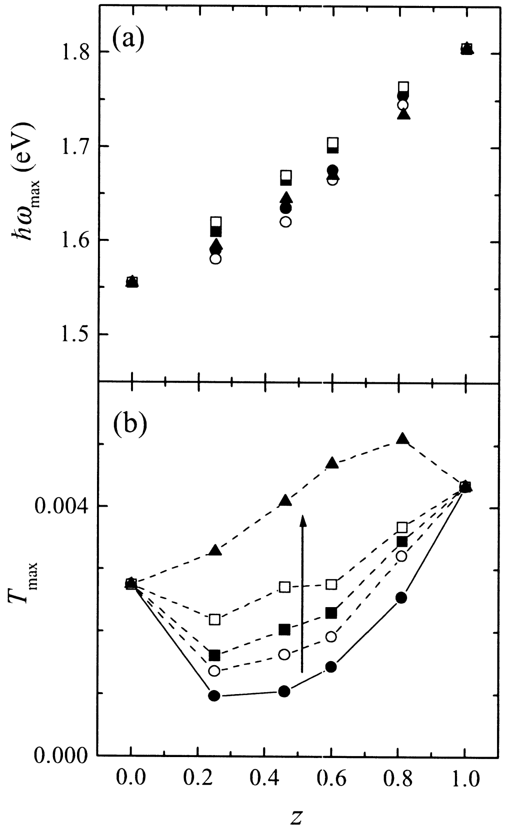

Fig. 5. The effect of the various Drude-Lorentz parameters on the z-dependence of $\hbar\omega_{max}$ and T_{max}. Solid circles: calculated from the DL parametrizations of $\varepsilon(\omega)$. Open circles: linear z-dependence assumed for τ (see dashed line in Fig. 6). Solid squares: additionally $\omega_{01}(z)$ and $\omega_{02}(z)$ linearized. Open squares: additionally $\beta_{01}(z)$ and $\beta_{02}(z)$ linearized. Solid triangles: all DL parameters in Fig. 6 linearized. See text for more details.

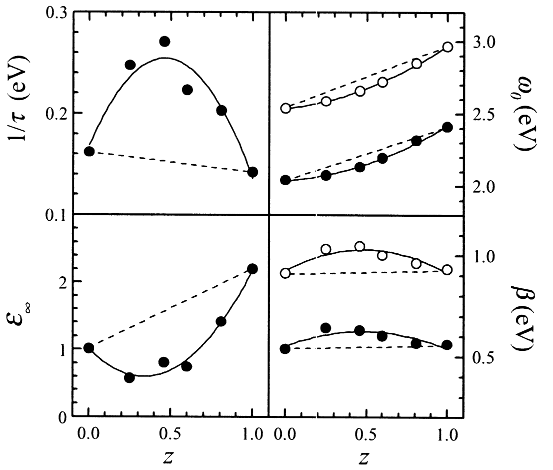

Fig. 6. Fit parameters for which the *z*-dependence exhibit a non-linear behavior. Apparently these parameters are affected by disorder.

broadening parameters $\beta_\mathrm{i}(z)$ of the first and second LO and $\tau(z)$ (see Fig. 6).

To study the effect of the non-linear *z*-dependence of these parameters on the dihydride transmission window, we calculate transmittance spectra assuming a linear dependence for $\tau(z)$ [see dashed line in Fig. 6(a)]. The resulting $T_\mathrm{max}(z)$ and $\hbar\omega_\mathrm{max}(z)$ are indicated by open circles in Fig. 5. We then additionally linearized $\omega_{0\mathrm{i}}$ for the first and second LO (solid squares) and subsequently also for $\beta_{0\mathrm{i}}$ (open squares). The resulting $T_\mathrm{max}(z)$ and $\hbar\omega_\mathrm{max}(z)$ with additionally $\varepsilon_\infty(z)$ linearized is given by solid triangles. Surprisingly, the main contribution to the suppression of the dihydride window comes from the non-linearity of ε_∞ ($\approx 40\%$). The other parameters τ, $\omega_{0\mathrm{i}}$ and β_i all contribute $\approx 20\%$ to the non-linear behavior of $T(z)$. With all *z*-dependences linearized, the suppression of the dihydride transmission does not occur. Note that the shift of $\hbar\omega_\mathrm{max}(z)$ is not affected.

4. Conclusions

In conclusion, the suppression of the dihydride window is due to atomic disorder via its influence on optical absorptions at energies larger than 4.5 eV. It is important to note that the suppression of the dihydride transmission window in $La_{1-z}Y_zH_x$ has a completely different origin than in the $Mg_{0.5}Y_{0.5}H_x$ system. As shown by Nagengast et al. [4] the latter system switches by first forming Mg and YH_2 clusters and then MgH_2 and YH_3 clusters. Although the YH_2 clusters are slightly transparent, the appearance of the whole film is highly reflective and non-transparent due to the presence of the metallic Mg clusters. Such a disproportionation does not occur in the $La_{1-z}Y_zH_x$ alloys.

We have strong indications that in *in*homogeneous La–Y alloys the dihydride transmission window is suppressed below $T = 10^{-5}$ (not presented here), which is interesting for switchable mirror applications, since it increases considerably the transmission contrast ratio between $La_{1-z}Y_zH_2$ and $La_{1-z}Y_zH_3$.

Acknowledgements

The authors thank M. van den Berg (VU Amsterdam) and P.A. Duine (Philips Research) for fruitful discussions. This work is part of the research program of the Stichting voor Fundamenteel Onderzoek der Materie (FOM), financially supported by the Nederlandse Organisatie voor Wetenschappelijk Onderzoek (NWO) and Philips Research, and of the TMR Research Network 'Metal-hydride films with switchable physical properties'.

References

[1] J.N. Huiberts, R. Griessen, J.H. Rector, R.J. Wijngaarden, J.P. Dekker, D.G. de Groot, N.J. Koeman, Nature (Lond.) 380 (1996) 231.

[2] P. van der Sluis, M. Ouwerkerk, P.A. Duine, Appl. Phys. Lett. 70 (1997) 3356.

[3] R. Griessen, J.N. Huiberts, M. Kremers, A.T.M. van Gogh, N.J. Koeman, J.P. Dekker, P.H.L. Notten, J. Alloys Comp. 253–254 (1997) 44.

[4] D.G. Nagengast, A.T.M. van Gogh, E.S. Kooij, B. Dam, R. Griessen, Appl. Phys. Lett. 75 (1999) 2050.

[5] R. Griessen, J.N. Huiberts, J.H. Rector, European Patent No. 0772795 (May 14, 1997) and US Patent No. 5,635,729 (June 3, 1997).

[6] A.T.M. van Gogh, S.J. van der Molen, J.W.J. Kerssemakers, N.J. Koeman, R. Griessen, Appl. Phys. Lett. 77 (2000) 815.

[7] P.H.L. Notten, M. Kremers, R. Griessen, J. Electrochem. Soc. 143 (1996) 3348.

[8] E.S. Kooij, A.T.M. van Gogh, R. Griessen, J. Electrochem. Soc. 146 (1999) 2990.

[9] A.T.M. van Gogh, D.G. Nagengast, E.S. Kooij, N.J. Koeman, J.H. Rector, R. Griessen, C.F.J. Flipse, R.J.J.G.A.M. Smeets, Phys. Rev. B 63 (2001) 195105.

[10] J.H. Weaver, R. Rosei, D.T. Peterson, Phys. Rev. B 19 (1979) 4855.

[11] D.J. Peterman, B.N. Harmon, J. Marchiando, J.H. Weaver, Phys. Rev. B 19 (1979) 4867.

[12] For the calculation we used the transfer matrix method. See for example O.S. Heavens, Optical Properties of Thin Solid Films (Butterworths, London, 1955).